BRET-based effector membrane translocation assay monitors GPCR-promoted and endocytosis-mediated G_q activation at early endosomes

Shane C. Wright[a,b], Viktoriya Lukasheva[b], Christian Le Gouill[b], Hiroyuki Kobayashi[b], Billy Breton[b], Samuel Mailhot-Larouche[b,c], Élodie Blondel-Tepaz[a,b], Nichelle Antunes Vieira[d], Claudio Costa-Neto[d], Madeleine Héroux[b], Nevin A. Lambert[e], Lucas Tabajara Parreiras-e-Silva[b,d,1], and Michel Bouvier[a,b,c,1]

[a]Department of Biochemistry and Molecular Medicine, Université de Montréal, Montréal, QC, H3T 1J4, Canada; [b]Institute for Research in Immunology and Cancer, Université de Montréal, Montréal, QC, H3T 1J4, Canada; [c]Molecular Biology Program, Université de Montréal, Montréal, QC, H3T 1J4, Canada; [d]Department of Biochemistry and Immunology, Ribeirão Preto Medical School, University of São Paulo, SP 14049-900, Brazil; and [e]Department of Pharmacology and Toxicology, Medical College of Georgia, Augusta University, Augusta, GA 30912

Edited by Brian K. Kobilka, Stanford University School of Medicine, Stanford, CA, and approved April 6, 2021 (received for review December 17, 2020)

G protein–coupled receptors (GPCRs) are gatekeepers of cellular homeostasis and the targets of a large proportion of drugs. In addition to their signaling activity at the plasma membrane, it has been proposed that their actions may result from translocation and activation of G proteins at endomembranes—namely endosomes. This could have a significant impact on our understanding of how signals from GPCR-targeting drugs are propagated within the cell. However, little is known about the mechanisms that drive G protein movement and activation in subcellular compartments. Using bioluminescence resonance energy transfer (BRET)–based effector membrane translocation assays, we dissected the mechanisms underlying endosomal G_q trafficking and activity following activation of G_q-coupled receptors, including the angiotensin II type 1, bradykinin B_2, oxytocin, thromboxane A_2 alpha isoform, and muscarinic acetylcholine M_3 receptors. Our data reveal that GPCR-promoted activation of G_q at the plasma membrane induces its translocation to endosomes independently of β-arrestin engagement and receptor endocytosis. In contrast, G_q activity at endosomes was found to rely on both receptor endocytosis-dependent and -independent mechanisms. In addition to shedding light on the molecular processes controlling subcellular G_q signaling, our study provides a set of tools that will be generally applicable to the study of G protein translocation and activation at endosomes and other subcellular organelles, as well as the contribution of signal propagation to drug action.

GPCR | endosomal signaling | Gq/11 | arrestin

G protein–coupled receptors (GPCRs) act as signaling hubs that direct molecular events to maintain cellular homeostasis. Historically, signal transduction has been thought to take place exclusively at the plasma membrane—where receptors activate heterotrimeric G proteins and β-arrestins (βARRs) desensitize them (1). This canonical view of receptor signaling has been challenged in recent years by observations that GPCRs can activate G proteins at endomembranes such as early endosomes, the Golgi apparatus, mitochondria, and the nucleus and that βARRs modulate signal amplitude and duration (2). These findings are important in the context of pharmacology and drug discovery because they will redefine how we understand cell signaling and may impact drug development in the future. Our understanding of the mechanisms controlling endomembrane signaling has been limited by the lack of tools required to quantitatively measure not only the presence of G protein but also their signaling at a subcellular level.

Studies aimed at better understanding G protein trafficking have largely focused on G_s, which is known to leave the plasma membrane upon activation, become cytoplasmic, and sample multiple endomembrane compartments (3, 4). Mechanistic insight into this phenomenon has revealed that G_s becomes reactivated at endosomes following translocation (5). However, less is known about the activation status of other G protein families found in subcellular organelles. In particular, G_q has been shown to transit from the plasma membrane to endosomes upon receptor activation and as a consequence of activating mutations (6–8). Yet, the contribution of βARR and receptor endocytosis to G protein trafficking and activation at endosomes has not been documented. In the absence of tools that directly measure G protein activation, current evidence for endosomal G_q activity has been limited to amplified downstream signaling events.

Nanobodies have been used as crystallization chaperones and as live cell imaging tools to visualize the distribution of active-state proteins (9). These tools have been particularly effective for G_s-coupled receptors in the absence of tools directly measuring the activity of the G protein in organelles (i.e., known effector regulators of G_s signaling). In particular, nanobodies or engineered G proteins that bind the active conformation of the receptor and nanobodies that stabilize the nucleotide-free state of G_s were used to suggest that receptor-G_s complexes were active

Significance

G protein–coupled receptors (GPCRs) have been proposed to signal in multiple compartments within the cell, a phenomenon that could have important implications for our understanding of receptor pharmacology and disease treatment. However, directly measuring G protein activity in subcellular compartments remains a challenge, and the mechanism underlying their translocation and activation remains elusive. Using a biosensor that specifically measures the presence of GTP-loaded $G_{q/11}$ at endosomes, our findings reveal the mechanism underlying G_q trafficking and signaling in the endosome and provide a powerful tool to directly monitor G protein movement and activation in subcellular compartments.

Author contributions: S.C.W., C.C.-N., M.H., N.A.L., L.T.P.-e.-S., and M.B. designed research; S.C.W., V.L., H.K., S.M.-L., E.B.-T., N.A.V., N.A.L., and L.T.P.-e.-S. performed research; V.L., C.L.G., B.B., N.A.L., and L.T.P.-e.-S. contributed new reagents/analytic tools; S.C.W., C.C.-N., M.H., N.A.L., L.T.P.-e.-S., and M.B. analyzed data; S.C.W., L.T.P.-e.-S., and M.B. wrote the paper; and S.C.W. and M.B. prepared figures for publication.

Competing interest statement: M.B. is the president of the scientific advisory board for Domain Therapeutics. V.L., C.L.G., B.B., and M.B. have filed patent applications related to the biosensors used in this work, and the technology has been licensed to Domain Therapeutics.

This article is a PNAS Direct Submission.

[1]To whom correspondence may be addressed. Email: lucastabajara@usp.br or michel.bouvier@umontreal.ca.

This article contains supporting information online at https://www.pnas.org/lookup/suppl/doi:10.1073/pnas.2025846118/-/DCSupplemental.

Published May 14, 2021.

at endomembranes (5, 10–12). In order to unearth more direct evidence of activation and a better understanding of the mechanisms for the other G protein families, tools that directly monitor the molecular events that immediately follow G protein activation would offer much-needed insight.

Enhanced bystander bioluminescence resonance energy transfer (ebBRET) was developed as a way to provide more sensitive and robust measurements of protein trafficking and activity in living cells. This technique relies on the natural association of the luciferase and green fluorescent protein (GFP) that both come from *Renilla reniformis* (*R*luc and rGFP, respectively). These two proteins do not interact spontaneously unless they are concentrated in the same compartment and thus can be used to monitor protein movement when the energy acceptor is anchored to a specific subcellular compartment (13). To measure the activity of G proteins at endosomes, we engineered an ebBRET-based effector membrane translocation assay (EMTA) for subcellular organelles. In addition, we developed organelle-targeted inhibitors to block G protein activity in a compartment-specific manner. Using these tools, we demonstrate the direct activation of $G_{q/11}$ by angiotensin II type 1 (AT_1R), bradykinin B_2 (B_2R), oxytocin (OXTR), thromboxane A_2 alpha isoform (TPαR), and muscarinic acetylcholine M_3 (M_3R) receptors in endosomes. Using cells devoid of βARRs (14), our results show that in contrast to the GPCRs, for which trafficking to endosomes is βARR-dependent, the trafficking of G_q to this compartment was not. These findings indicate that G_q translocation can occur through nonconventional receptor endocytosis–independent pathways. Interestingly, activation of G_q in the endosomal compartment was two-tiered, displaying a component that was βARR-independent and another that was further promoted by βARR, supporting the notion that the formation of a receptor–G_q complex in endosomes can promote G protein activation. Moreover, we show that G_q signaling at the plasma membrane not only exhibits a faster onset than the signaling that takes places in endosomes, but it is also functionally different. We anticipate that our methodological advances and mechanistic understanding of endosomal G_q signaling will be of general interest to the study of other GPCRs and to the study of G protein signaling in other compartments.

Results

Active Receptor and Active G_q Are Enriched in Early Endosomes following Agonist Stimulation. We set out to map the movement of active GPCRs and G_q proteins subsequent to stimulus at the plasma membrane. First, we employed mini-G (mG) proteins as a tool to monitor the distribution of active-state GPCRs following agonist stimulation of AT_1R in HEK293 cells. Confocal microscopy revealed that Venus-tagged mGsq (V-mGsq) (12) was located diffusely to the cytoplasm under basal conditions and translocated to plasma membrane upon receptor activation with angiotensin II (AngII, 100 nM). Subsequently, small vesicles containing V-mGsq were found and identified as early endosomes, as evidenced by colocalization with Cerulean-RAB5A (Fig. 1*A* and *SI Appendix*, Fig. S1). These observations were confirmed by employing plate reader–based ebBRET between *Renilla* luciferase (*R*luc8)–tagged mGsq and energy acceptors that were anchored to either the plasma membrane (rGFP-CAAX; polybasic sequence with the prenylated CAAX box of the GTPase first identified in Kirsten Rat Sarcoma virus [KRAS]) or early endosomes (rGFP-FYVE; zinc finger domain of endofin, which binds phosphatidylinositol 3-phosphate [PI3P]) as previously validated by confocal microscopy (13). Concentration response curves confirmed the translocation of mGsq to both the plasma membrane and early endosomes following receptor stimulation (Fig. 1*B*). We confirmed the presence of full-length G_q at the plasma membrane by calculating the netBRET of luciferase-tagged G_q in combination with acceptor-tagged markers of different cellular compartments; minimal BRET was observed at early endosomes, Golgi apparatus, endoplasmic reticulum, and mitochondria (*SI Appendix*, Fig. S2*A*). We then proceeded to use spectrometric BRET measurements to monitor G_q movements at the plasma membrane, early endosomes, and mitochondria. Stimulation of AT_1R resulted in a decrease in BRET at the plasma membrane and an increase in BRET at early endosomes, suggesting that G_q quickly leaves the membrane once activated and translocates to early endosomes (Fig. 1*C* and *SI Appendix*, Fig. S2*B*). In contrast, activation of AT_1R did not lead to an enrichment of G_q at mitochondria (rGFP-Bcl-xL) (*SI Appendix*, Fig. S2*B*). These results were reproduced with both B_2R and OXTR, indicating that this is a general mechanism for activated G_q (*SI Appendix*, Fig. S2 *C* and *D*). Parallel experiments employed luminescence microscopy to ascertain that G_q localized to the plasma membrane under basal conditions (*SI Appendix*, Fig. S3). We then coupled this technique with BRET imaging (15) to show that upon stimulation of AT_1R with AngII, G_q moved to early endosomes as measured by the increase in BRET when using rGFP-FYVE as an energy acceptor (*SI Appendix*, Fig. S3). These experiments unequivocally show that these vesicle-like structures are early endosomes that become enriched with G_q following AT_1R activation at the plasma membrane.

Traditional readouts to infer G_q activity have relied on conformational changes/dissociation within the heterotrimer or the use of downstream and, in some cases, signal-amplified responses such as PKC recruitment, IP_1 accumulation, Ca^{2+} mobilization, or ERK1/2 activation (16). We recently developed an effector-based toolbox for measuring direct activation of $G_{q/11}$, $G_{i/o}$, and $G_{12/13}$ in living cells (17). Adapting effector molecules to probe for subcellular G protein signaling offers the following advantages: 1) neither the receptor nor the G protein need to be modified, 2) effector molecules bind directly to the guanosine triphosphate (GTP)-bound Gα protein, and 3) the signal is not diffuse as in the case of signal amplified second messengers and kinase cascades. In order to create a biosensor that detects the active $G_{q/11}$ family, we generated a luciferase-tagged construct of the effector p63RhoGEF that only harbors its G protein–binding domain. When coexpressed with compartment-specific energy acceptors (i.e., rGFP-CAAX or rGFP-FYVE), subcellular G protein activation can be monitored. In order to determine the sensitivity of this biosensor, we expressed p63RhoGEF-*R*lucII with either rGFP-CAAX or rGFP-FYVE in HEK 293 cells expressing AT_1R (*SI Appendix*, Fig. S4*A*). In the absence of overexpressed G proteins, stimulation of AT_1R with AngII resulted in an increase in BRET, both at the plasma membrane and at early endosomes, indicating that this biosensor is sensitive enough to measure the activity of endogenous G proteins (*SI Appendix*, Fig. S4*B*). Heterologous expression of heterotrimeric G_q promoted a larger agonist-induced BRET response for both the plasma membrane and early endosomes (Fig. 1*D* and *SI Appendix*, Fig. S4*B*). As expected, G_q activation at the plasma membrane was faster ($t_{1/2}$ ~12.5 s; 95% CI: 11.2 to 13.9 s) when compared to the endosomal activation ($t_{1/2}$ ~56.4 s; 95% CI: 44.7 to 73.5 s) (Fig. 1*D* and *SI Appendix*, Fig. S4*B*). Recruitment of p63RhoGEF to either compartment was reversible using the AT_1R-specific and competitive antagonist Losartan, and similar disparities in time were observed (rGFP-CAAX: $t_{1/2}$ ~358.5 s; 95% CI: 336.1 to 383.9 s and rGFP-FYVE: $t_{1/2}$ ~1,107 s; 95% CI: 580.5 to 1,214 s). The longer response observed at endosomes after Losartan treatment is most likely multifactorial and may include 1) ligand-receptor interaction, 2) intrinsic GTPase activity of the G protein, and 3) relative abundance of regulators of G protein signaling (RGS) proteins in the different compartments. In addition, given a logP of 1.19 at pH 7, Losartan should be relatively membrane permeable. Yet, its partition between the extracellular milieu and the endosomal lumen requires permeating two lipidic membranes. This most likely delays the equilibration of the Losartan concentration between the compartments that, independently of the other components noted above, would affect the observed inactivation kinetics.

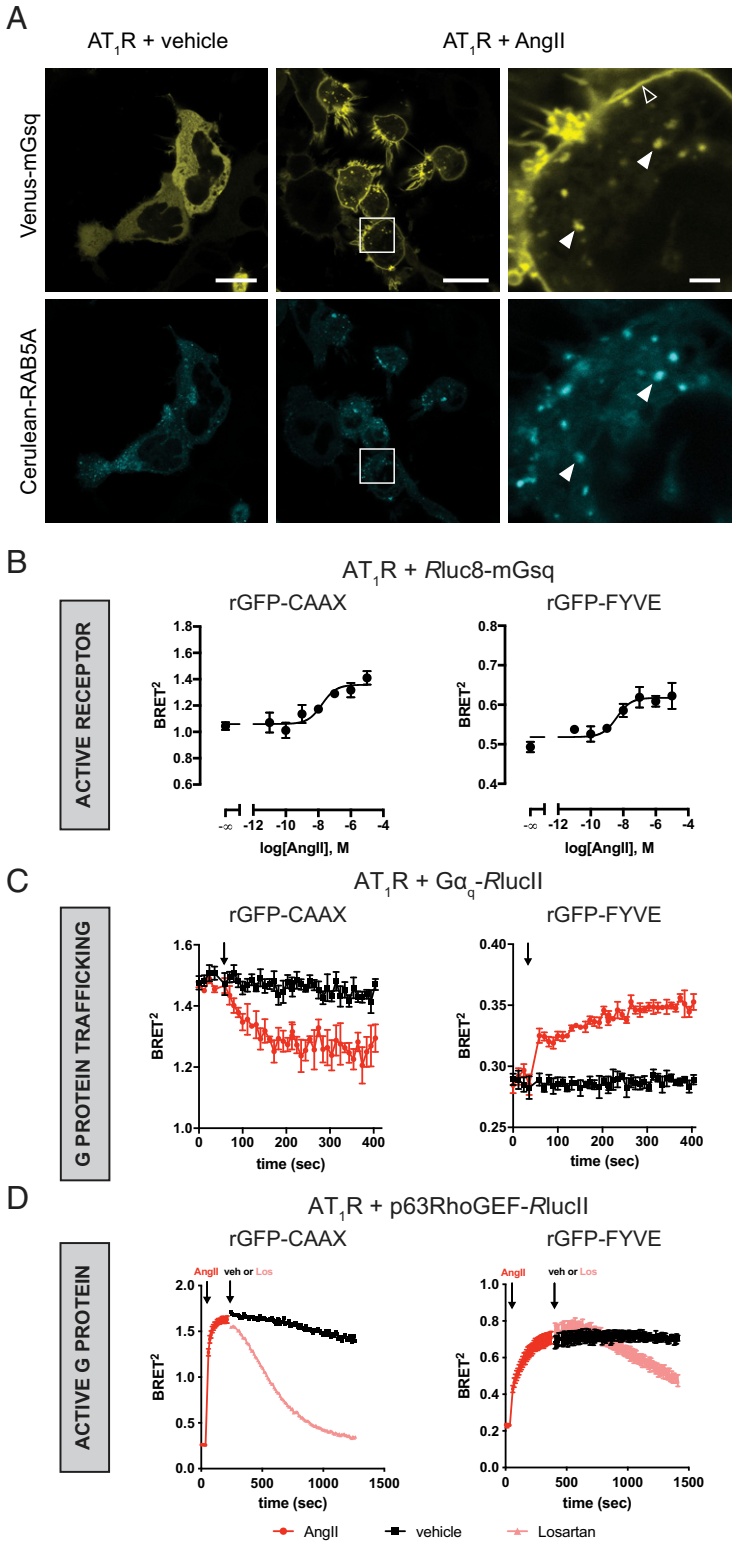

Fig. 1. Active receptor and active G_q are enriched in early endosomes following stimulation. (*A*) AT_1R remains active in early endosomes. Confocal images of HEK 293 cells expressing AT_1R, NES-Venus-mGsq and Cerulean-RAB5A and exposed to vehicle or AngII for 15 min. NES-Venus-mGsq is recruited to active AT_1R at the plasma membrane (open arrowhead) as well as RAB5A-positive early endosomes (closed arrowheads). Images are representative of 15 cells from three independent experiments. (*B*) Plate reader–based ebBRET between mGsq-*R*luc8 and either rGFP-CAAX or rGFP-FYVE following stimulation of AT_1R. Data are represented as the mean ± SEM ($n = 3$). (*C*) Plate reader–based ebBRET between $G\alpha_q$-118-RlucII and either rGFP-CAAX or rGFP-FYVE following stimulation of AT_1R with either vehicle (black) or AngII (red) using an injector. Data are represented as the mean ± SEM ($n = 3$ to 4). (*D*) Activation of G_q at the plasma membrane and early endosomes after AT_1R stimulation with AngII (50 nM) using an injector. The reversible nature of the interaction between the p63RhoGEF sensor and G_q was demonstrated by injection of the antagonist Losartan (10 μM). Data are represented as the mean ± SEM ($n = 3$ to 7). (Scale bars, 20 μm [*Left and Center*] and 2 μm [*Right*].)

The generality of endosomal G_q signaling was confirmed by measuring B_2R- and OXTR-mediated G_q activation at the plasma membrane and early endosomes (*SI Appendix*, Fig. S4 *C* and *D*). Using luminescence and BRET microscopy, we were able to visualize the redistribution of cytosolic p63RhoGEF to the plasma membrane and early endosomes (*SI Appendix*, Fig. S5 and Movie S1). Further characterization of AT_1R through selective inhibition of $G_{q/11}$ with the pharmacological inhibitor YM-254890 (*SI Appendix*, Fig. S6 *A* and *B*) and stimulation with the βARR-biased agonist TRV027 (*SI Appendix*, Fig. S6 *C–E*) confirmed that p63RhoGEF could be used as a tool to selectively detect activation of the $G_{q/11}$ family.

p63RhoGEF Detects the Activation of $G_{q/11}$ Paralogues in Endosomes. The $G_{q/11}$ family of Gα subunits consists of G_q and G_{11} that are ubiquitously expressed and G_{14} and G_{15} that are more limited in expression (18). p63RhoGEF has been shown to selectively bind to all active Gα proteins of the $G_{q/11}$ family (17, 19, 20). We applied this tool to probe for the ability of AT_1R, M_3R, and TPαR to signal through $G_{q/11}$ paralogues at the plasma membrane and at early endosomes (Fig. 2 *A–C*). While G_q, G_{11}, G_{14}, and G_{15} were activated at the plasma membrane by all receptors, albeit at different potencies and efficacies, activation in early endosomes varied considerably. For example, M_3R activated all paralogues at endosomes, while TPαR activated G_q and G_{11}, but not G_{14} or G_{15}. Whether this results from an overall lower activation of G_q by TPαR compared to M_3R or a difference in the subcellular activation of the paralogues remains to be investigated. In the case of TPαR, given that the level of activation of G_{14} at the plasma membrane was similar to that of G_q, the absence of G_{14} activation at endosomes compared to the robust activation of G_q suggests that there are receptor intrinsic differences. The selectivity of the sensor was confirmed by the observation that heterologous expression of $G_{12/13}$ did not promote p63RhoGEF recruitment after stimulation of AT_1R. In fact, a competition between $G_{12/13}$ and endogenous G_q for the receptor could be observed by the decrease in recruitment (Fig. 2*A*). The AngII-promoted p63RhoGEF recruitment observed in the absence of overexpressed G proteins indicates that the biosensor can be used to monitor activity of native signaling components. The fact that such an endogenous activity could be detected with AT_1R, but not M_3R and TPαR, may emphasize the importance of the relative stoichiometry of the signaling components. Taken together, these differences highlight the diversity of endosomal $G_{q/11}$ activity and suggest that there are more profound differences in the signaling that takes place at the plasma membrane and endosomes.

βARR-Mediated Endocytosis Enhances $G_{q/11}$ Signaling in Endosomes. Sustained GPCR-mediated signaling in early endosomes is thought to depend on βARR-mediated receptor endocytosis, but it is not clear whether this governs $G_{q/11}$ trafficking and to what extent the second wave of signaling is dependent on the presence of internalized receptors. To this end, we monitored AT_1R internalization, G_q trafficking, and activation in HEK 293 cells and cells lacking βARR engineered by CRISPR/Cas9 (ΔβARR cells) (14). ebBRET experiments employing rGFP-FYVE as an endosomal marker revealed robust enrichment of AT_1R, G_q, and p63RhoGEF after prolonged agonist treatment (Fig. 3 *A–C*). Internalization of AT_1R is dependent on βARR-mediated endocytosis, and the absence of βARR prevented accumulation of AT_1R in endosomes following agonist stimulation (Fig. 3*A*). In ΔβARR cells, activation of G_q at the plasma membrane was unaffected compared to parental cells, while endosomal activation was partially inhibited (Fig. 3*C*), suggesting that receptor-mediated activation of G_q at endosomes plays a part in the endosomal response. In contrast to p63RhoGEF, translocation of G_q to endosomes was not dependent on βARR (Fig. 3*B*). We confirmed these observations by carrying out similar experiments with M_3R (*SI Appendix*, Fig. S7). While the lack of βARR did not have an effect on the trafficking of G_q to endosomes (*SI Appendix*, Fig. S7*B*) nor on its activation at the plasma membrane (*SI Appendix*, Fig. S7 *C*, *Left*), βARR was in part required for endosomal activation of G_q (*SI Appendix*, Fig. S7 *C*, *Right*). Collectively, our results suggest that GPCR internalization, via βARR-dependent routes, promotes G_q activation at early endosomes. Further work will be needed to determine whether the residual endosomal G_q response observed in ΔβARR cells results from receptors that are less dependent on βARR for internalization or from long-lasting activity of G_q in the absence of receptor.

Prevention of Endosomal Acidification Increases $G_{q/11}$ Activity. The pH of endosomes becomes acidic during the endocytic process because of the activity of vacuolar-type H^+-ATPase (V-ATPase). pH modification has been shown to affect the off rate of the ligand for receptors (21, 22). To confirm that agonist-bound receptors contribute to endosomal G_q signaling, we used bafilomycin that binds to V-ATPase and prevents endosomal acidification (23, 24). As expected, activation of G_q by AT_1R at the plasma membrane was not affected by bafilomycin (Fig. 4 and *SI Appendix*, Fig. S8, *Left*). In contrast, preincubating cells with bafilomycin resulted in an increase in the activation of G_q in early endosomes mediated by AngII-bound AT_1R (Fig. 4 and *SI Appendix*, Fig. S8, *Right*), consistent with the blockade by Losartan (Fig. 1*D*). However, given that bafilomycin can also affect endosomal maturation (24), we cannot exclude that the observed effect may result from a direct action on the endosomes.

Activation of $G_{q/11}$ at the Plasma Membrane Is Required for Subsequent Endosomal Activation. Once activated, G proteins have intrinsic GTPase activity that allows for the hydrolysis of GTP to guanosine diphosphate (GDP). This process is accelerated by proteins known as GTPase-activating proteins or RGS proteins in a way that is specific to G protein families (25–28). We hypothesized that subcellular activation of $G_{q/11}$ could be selectively targeted through the generation of organelle-specific inhibitors. By tethering the RGS domain of GRK2 to either the plasma membrane (RGS-CAAX) or endosomes (RGS-FYVE), we generated $G_{q/11}$-specific tools to manipulate their activity in subcellular compartments (Fig. 5*A*). We sought to test the effect of these tools on the activation of heterotrimeric G_q by AT_1R. AT_1R-mediated activation of G_q at the plasma membrane was largely inhibited by RGS-CAAX expression, but not RGS-FYVE, when measuring the BRET between p63RhoGEF-*R*lucII and rGFP-CAAX (Fig. 5*B*). This was in contrast to early endosomes, where both RGS-CAAX and RGS-FYVE expression abolished the activation of $G_{q/11}$ (Fig. 5*C*). This was not due to differences in protein expression at the plasma membrane, since no difference was observed for AT_1R and G_q, which are both localized to the plasma membrane under basal conditions (*SI Appendix*, Fig. S9 *A* and *B*). Organelle-specific inhibitors were also used in the characterization of B_2R and OXTR-mediated G_q signaling, and similar profiles were observed (*SI Appendix*, Fig. S9 *C* and *D*). Collectively, these results suggest that G protein activation at the plasma membrane is required for subsequent activation at early endosomes.

Endosomal Activation of $G_{q/11}$ Signaling Is Intrinsically Different from Plasma Membrane Activation. While p63RhoGEF can be used as a tool to indiscriminately measure $G_{q/11}$ activation in different compartments, it does not provide information about the molecular differences with respect to signaling at the plasma membrane and endosomes, other than the fact that they are kinetically dissimilar. In order to address these possible differences, we further characterized the activation of protein partners of G_q immediately downstream of its own activation. Heterotrimer dissociation is an

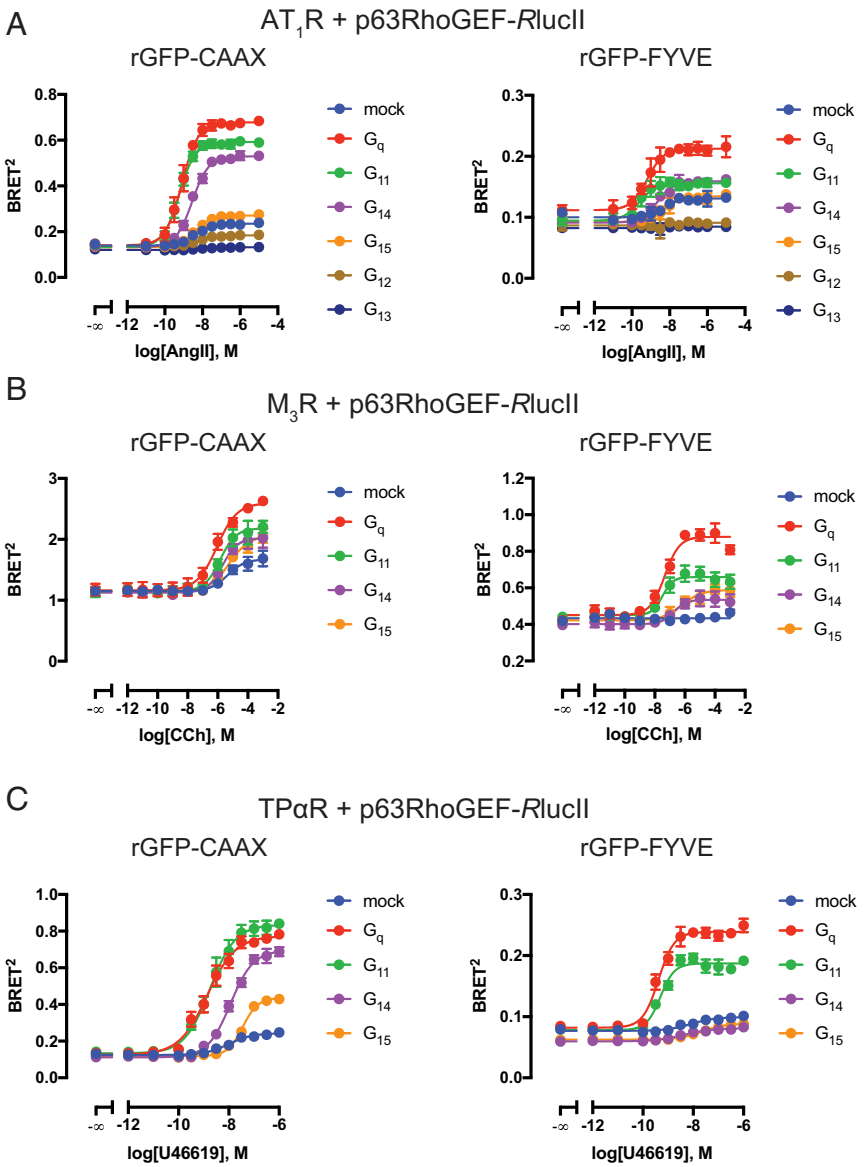

Fig. 2. p63RhoGEF detects the activation of $G_{q/11}$ paralogues in endosomes. (*A*–*C*) Activation of endogenous $G_{q/11}$ and overexpressed G_q, G_{11}, G_{14}, or G_{15}, at the plasma membrane or at early endosomes following stimulation of AT_1R (*A*), M_3R (*B*), or TPαR (*C*). Data are represented as the mean ± SEM (n = 3 to 8).

important step in triggering signaling cascades downstream of G_q activation. GRK2 is known to localize to the cytosol under basal conditions and is recruited to the plasma membrane following the release of Gβγ, where it mediates receptor desensitization (29). On the other hand, Gβγ has been shown to participate in distinct signaling pathways and regulates the activity of ion channels, G protein–gated inward rectifier channels, and adenylyl cyclase (30, 31). In order to measure the release of Gβγ, we employed a mutant of GRK2 that does not bind active $G\alpha_q$ (GRK2-D110A) (32). Stimulation of AT_1R with AngII led to robust responses at both the plasma membrane and early endosomes (Fig. 6*A*). Recruitment of GRK2-D110A to both compartments was also observed after stimulation of M_3R (*SI Appendix*, Fig. S10). In contrast, the production of diacylglycerol (DAG) by phospholipase C β activation, as measured by *R*lucII-C1B (DAG-binding domain of PKCδ) recruitment, was restricted to the plasma membrane and not detectable at early endosomes (Fig. 6*B* and *SI Appendix*, Fig. S11), consistent with PIP_2 being restricted to the plasma membrane. These findings are expected but emphasize the unique nature of endosomal G_q activity while confirming the specificity of our endosomal marker. Further work is required to uncover the mediators of endosomal G_q signaling and to reveal what the associated functional consequences are.

Discussion

In recent years, high-throughput screening efforts have relied on endpoint readouts that are often signal amplified and do not delineate the contributions of the signaling components (i.e., receptor/G protein/βARR). Increasingly, functional selectivity (biased signaling) at the level of the individual G proteins and βARR paralogues is starting to be considered, but not within the context of subcellular localization. The advent of GPCR and G protein–targeted nanobodies has facilitated a better understanding of the biology in living cells (9). Probing the prototypical β_2-adrenergic receptor with these tools revealed that canonical GPCR activation and nucleotide exchange of heterotrimeric G_s may occur in early

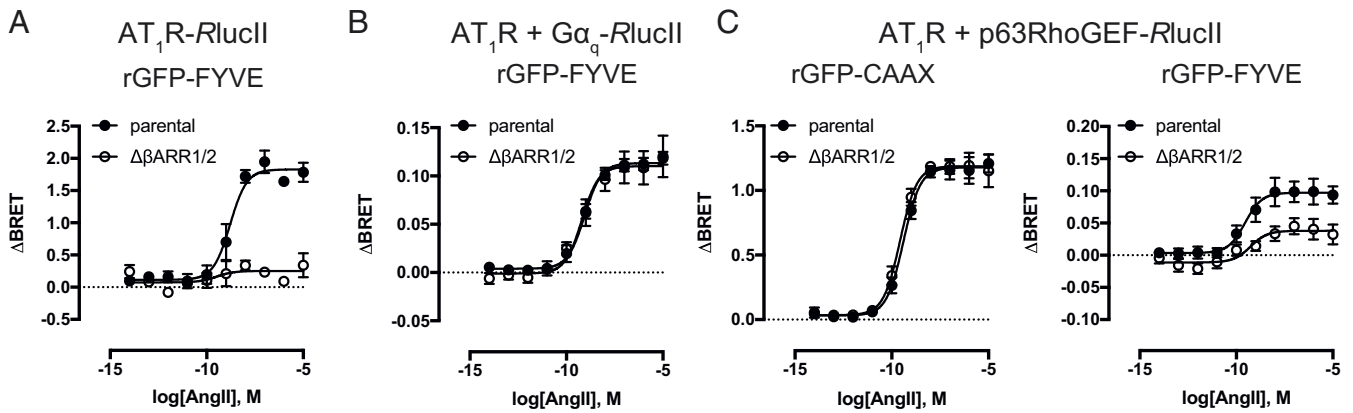

Fig. 3. Endocytosed receptor and β-arrestin contribute to $G_{q/11}$ signaling in endosomes. (*A*–*C*) Trafficking of AT_1R (*A*) and G_q (*B*) to endosomes and detection of G_q activation (p63RhoGEF, *C*) at the plasma membrane and early endosomes was measured by ebBRET in parental HEK 293 and ΔβARR cells using luciferase-tagged versions of the aforementioned proteins and either rGFP-CAAX or rGFP-FYVE as an energy acceptor following AT_1R stimulation with AngII. Data are represented as the mean ± SEM (n = 3 to 8); also see *SI Appendix*, Fig. S4.

endosomes in addition to the plasma membrane (5, 33). These findings challenged the traditional model of receptor desensitization and revealed that GPCR signaling is more complex than previously thought. Negative-stain electron microscopy, single-particle electron microscopy, and cryogenic electron microscopy revealed the mechanism through which GPCR-G protein-βARR megaplexes exist and allow for sustained G protein signaling (34–36). Some of these structural biology tools have been repurposed as biosensors, such as the nanobodies used to stabilize either the receptor or nucleotide-free G protein or the mG proteins used to detect and stabilize the active receptor conformation (5, 10, 12). These tools have largely focused on the subcellular signaling of G_s-coupled receptors and do not directly measure the active G protein (GTP-bound) or effector recruitment to subcellular organelles. In the current study, we demonstrate that the ebBRET-based approach EMTA can be used to measure the activation of G_q in endosomes through biosensor expression of the G_q-regulated RhoGEF, p63RhoGEF.

Activated G_q is an important mediator in signal transduction, interacting with PLCβ, GRK2, and p63RhoGEF (37). Of particular interest, p63RhoGEF is basally autoinhibited and activated by GTP-bound G_q to exert its function as a guanine nucleotide exchange factor for RhoA, RhoB, and RhoC (20). Whereas RhoA localizes to the plasma membrane and plays a role in the regulation of cytoskeletal reorganization, cell shape change, and protein trafficking, RhoB is enriched in endosomes and inhibits the transport of endosomal cargo to lysosomes (38). In light of these previous findings, our observations that G_q can be activated at endosomes in addition to the plasma membrane suggest that compartmentalized G_q signaling is not equivalent and could result in different biological outcomes.

Endosomal G_q has been proposed to play a physiological role in the exacerbation of a number of diseases for which novel treatments are being sought (6, 8). However, previous studies did not investigate the trafficking route of G_q, monitor G_q activity directly, or dissect the relative contribution of the different components (receptor, G protein, and βARR) leading to endosomal activity. Moreover, traditional tools for studying endosomal signaling are based on inhibition of receptor-mediated endocytosis using inhibitors of dynamin or clathrin. Given that these small-molecule inhibitors prevent receptor complex internalization, they do not only block G protein–mediated signaling from endosomes, but they also prevent βARR-dependent signaling. The observation that G_q translocates to endosomes in the

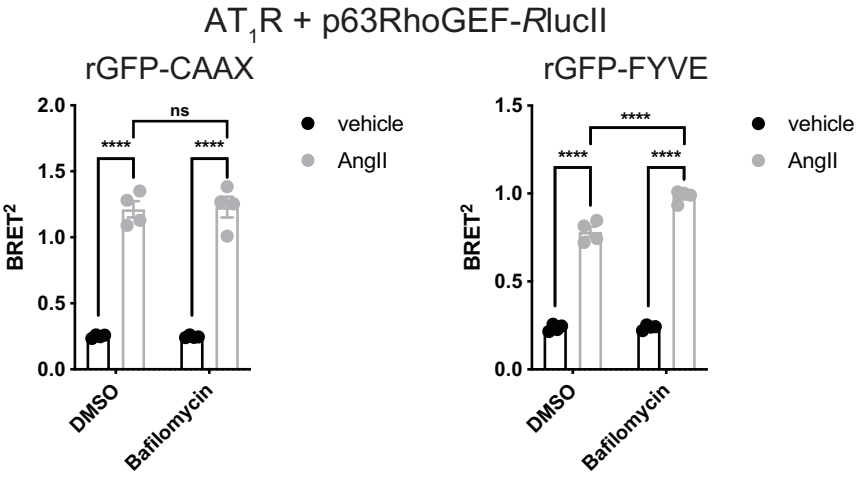

Fig. 4. Prevention of endosomal acidification increases $G_{q/11}$ activity. Activation of G_q at the plasma membrane and early endosomes following incubation with bafilomycin (1 μM) and stimulation with AngII (100 nM). Data are represented as the mean ± SEM (n = 4). ns, nonsignificant; ****P < 0.0001 (two-way ANOVA).

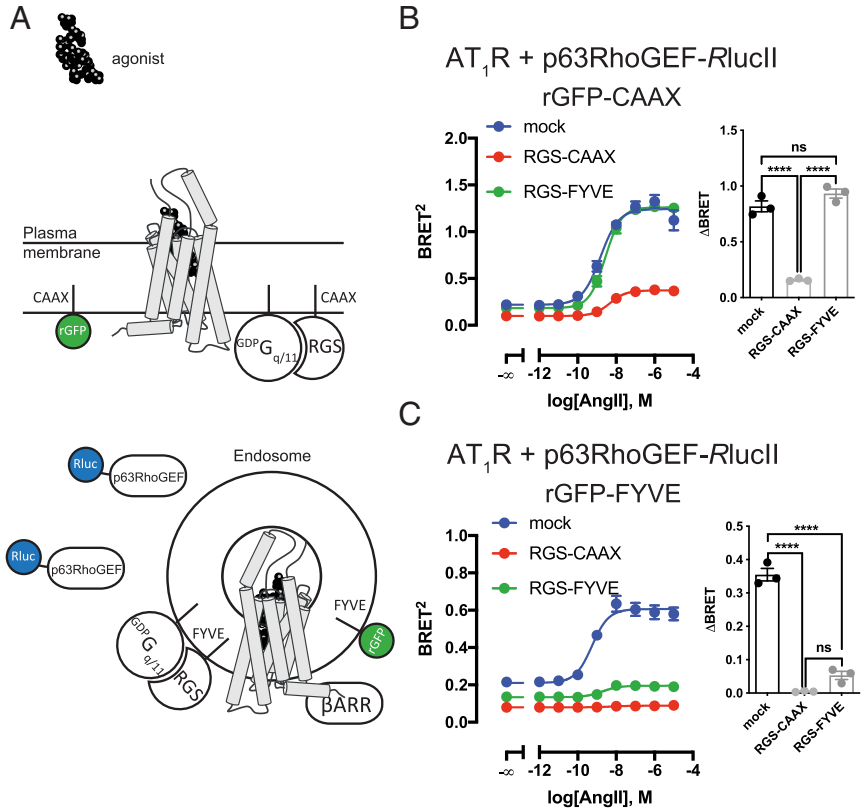

Fig. 5. Activation of $G_{q/11}$ at the plasma membrane is required for subsequent activation at early endosomes. (*A*) Schematic representation of the inhibition of $G_{q/11}$ activity in subcellular compartments by tethering the RGS domain of GRK2 to either the plasma membrane (RGS-CAAX) or endosomes (RGS-FYVE), preventing recruitment of p63RhoGEF in the absence of GTP-bound $G_{q/11}$. (*B* and *C*) Concentration response curves demonstrate the use of membrane-tethered RGS and endosomal RGS to modulate activation of heterotrimeric G_q by AT_1R at the plasma membrane (*B*) or in endosomes (*C*). Bar graphs depict the ligand-induced differences when AT_1R was stimulated with 100 nM AngII. Data are represented as the mean ± SEM ($n = 3$). ns, nonsignificant; ****$P <$ 0.0001 (one-way ANOVA).

absence of βARR suggests that part of its trafficking includes cytoplasmic release followed by probing of endomembranes, including endosomes—a mechanism that parallels what has been proposed for G_s trafficking to endosomes (3, 4, 39, 40). In order to pinpoint the activation of heterotrimeric G proteins in endosomes, we developed organelle-specific inhibitors based on the RGS domain of GRK2. These tools can be localized to different compartments within the cell using organelle-specific markers. Our data suggest that G_q activation at endosomes requires a primary activation event at the plasma membrane. The presence of the receptor in endosomes further promotes the activation of these G_q molecules in addition to the GTP-bound G_q that arrives at endosomes independently of receptor endocytosis. It remains to be seen if βARR stabilizes the complex in endosomes as it does in the case of the G_s-containing megaplex (34). Intuitively, one would deduce that the distribution of the aforementioned receptor complexes in endosomes likely depends on ligand bias and the intrinsic ability of the receptor to interact with βARR (i.e., Class A/Class B GPCR).

Our findings reinforce recent advances on the consequences of bias. The fact that the conformational landscape of a given GPCR can be stabilized by a particular ligand to favor distinct allosteric sites that preferentially interact with one effector over another has implications for sustained signaling responses, a concept known as kinetic bias (41). In the case of AT_1R, TRV027 drives the receptor into a conformation that favors the recruitment of βARR while preventing both membrane and endosomal activation of G_q. Different approaches have been used to maintain plasma membrane signaling while preventing a second wave of signaling in endosomes. Engineered drugs that rely on the acidic pH of early endosomes such as pH-responsive nanoparticles and hydrophobic tags have enabled directed inactivation of endosomal GPCRs; however, it remains unclear what the functional consequences for antagonizing both G proteins and βARR in endosomes are (8, 42). More specifically, how would shifting the balance between GPCR-βARR and GPCR-G protein complexes in endosomes affect the biology of cellular responses? Selectively targeting RGS proteins to specific subcellular domains as we have done in this study could begin to answer this question. The level of detail with which we are able to measure signaling responses in living cells has substantially increased with advances in our technological repertoire, and this has profound implications for the 30 to 40% of drugs that target GPCRs in the clinic. In summary, we present engineered BRET-based endosomal signaling biosensors that unequivocally show the presence of GTP-bound G_q at endosomes through a mechanism resulting from G protein trafficking that is receptor endocytosis–independent and whose activity is either self-sustained or enhanced by endocytosed receptors. Extension of these tools to native tissues will provide a better understanding of endosomal signaling under physiological and pathological conditions and may reveal receptor- and cell-specific differences that impact subcellular signaling.

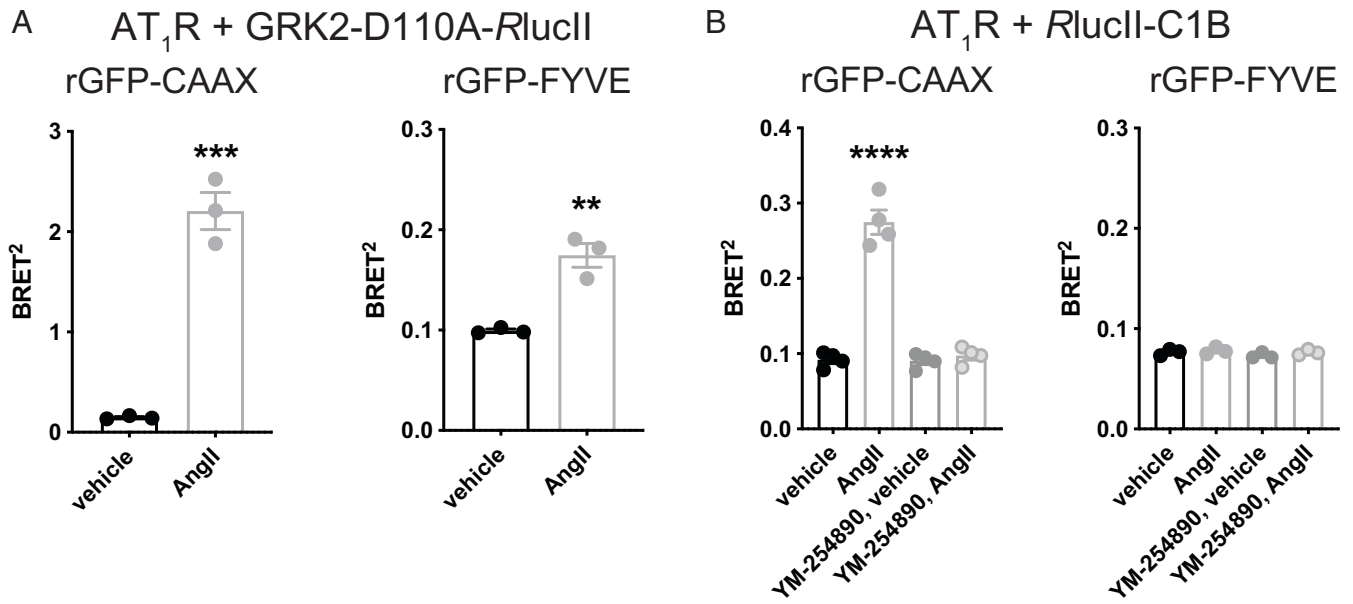

Fig. 6. Endosomal activation of $G_{q/11}$ signaling is intrinsically different from plasma membrane activation. (*A*) ebBRET between GRK2-D110-*R*lucII and rGFP-CAAX or rGFP-FYVE following stimulation of AT_1R with AngII (10 μM). Data are represented as the mean ± SEM ($n = 3$). $^{**}P < 0.01$; $^{***}P < 0.001$ (unpaired *t* test). (*B*) ebBRET between *R*lucII-C1B and rGFP-CAAX or rGFP-FYVE following AT_1R stimulation with AngII (100 nM), in the presence or absence of G_q inhibitor YM-254890 (1 μM). Data are represented as the mean ± SEM ($n = 3$ to 4). $^{****}P < 0.0001$ (one-way ANOVA).

Materials and Methods

Reagents. Dulbecco's phosphate-buffered saline (D-PBS), Dulbecco's modified Eagle's medium (DMEM), Trypsin, PBS, penicillin/streptomycin, fetal bovine serum, and newborn calf serum were from Wisent Bioproducts. Polyethylenimine (PEI) was purchased from Alfa Aesar (Thermo Fisher Scientific), and X-tremeGENE 9 transfection reagent as well as acetylcholine chloride (ACh), bovine serum albumin, bradykinin acetate salt, and carbamoylcholine chloride were from Sigma-Aldrich. AngII was either from Sigma-Aldrich or GenScript; Losartan was from Fagron; oxytocin acetate, U46619, and bafilomycin were from Cayman Chemical; TRV027 was from Trevena; and YM-254890 was from Wako Pure Chemical Industries. Coelenterazine 400a, coelenterazine h, and Prolume Purple were purchased from Nanolight Technologies.

Plasmid DNA Constructs. M_3R-*R*luc8 (12), FLAG-AT_1R (43), HA-TPαR (44), $Gα_q$-118-*R*lucII (45), p63RhoGEF-*R*lucII (17), GRK2-D110A-*R*lucII (46), βARR2-*R*lucII (47), AT_1R-*R*lucII, rGFP-CAAX, and rGFP-FYVE (13) have been described previously. B_2R, HA-M_3R, OXTR, $Gα_q$, $Gα_{11}$, $Gα_{14}$, $Gα_{15}$, $Gβ_1$, $Gγ_{1,}$ $Gγ_{2,}$ and $Gγ_5$ were purchased from cDNA.org (Bloomsburg University). *R*luc8-mGsq was obtained by excising a fragment encoding mGsq from NES-Venus-mGsq (12) with XhoI and EcoRI and ligating into *R*luc8-C1. To target the RGS domain from GRK2 to the plasma membrane and to early endosomes, the RGS was PCR amplified and subcloned as follows. 1) tdFYVE-RGS(GRK2): pcDNA3.1 tdFYVE-*R*lucII was digested with HindIII and ApaI to replace *R*lucII with the RGS domain using Gibson assembly, and 2) RGS(GRK2)-CAAX: pcDNA3.1 rGFP-CAAX (Kras) and the PCR amplicon were digested with NheI and BamHI and ligated to replace rGFP with the RGS domain. For the *R*lucII-C1B (DAG-binding domain of PKCδ) construct, the C1B coding sequence was excised using BamHI + PmeI from a BRET-based PKC sensor (48), subcloned in pcDNA3.1 (+) *R*lucII-GFP10, and digested with the same restriction enzymes, replacing GFP10 by C1B. The constructs encoding different cellular compartment markers were created using cDNA fragments synthesized at GeneArt (ThermoFisher): a marker of the Golgi apparatus, pcDNA 3.1 Zeo (+) tdrGFP-Golgi (Giantin: 3131–3259); an endoplasmic reticulum (ER) marker, pcDNA 3.1 (+) tdrGFP-ER (PTP1B: last 27-Cterm); and a marker for mitochondria, pcDNA3.1 (+) rGFP-mito (Bcl-xL). One DNA fragment encoding the previously reported (3) Golgi-targeting domain of Giantin (EPQQSFSEAQQQLCNTRQEVNELRKLLEEERDQRVAAENALSVAEEQIRRLEHSEWDSSRTPIIGSCGTQEQALLIDLTSNSCRRTRSGVGWKRVLRSLCHSRTRVPLLAAIYFLMIHVLLILCFTGHL) was subcloned by Gibson assembly in pcDNA3.1 Zeo (+) tdrGFP-GNG5, digested with KpnI + XbaI, creating the rGFP-tagged Golgi marker. This DNA fragment also encoded the ER-targeting domain of PTP1B (FLVNMCVATVLTAGAYLCYRFLFNSNT), isolated from the Giantin sequence by three stop codons in different reading frames. This construct was then digested with KpnI to excise the Giantin coding sequence with internal stop codons, leaving the PTP1B coding sequence in frame with the tdrGFP and creating the rGFP-tagged ER marker. For the mitochondrial rGFP-tagged marker, the DNA fragment encoding a sequence from Bcl-xL (RKGQERFNRWFLTGMTVAGVVLLGSLFSRK) was subcloned by Gibson assembly in pcDNA3.1 (+) rGFP-CAAX(kras) digested with EcoRI + BamHI. All plasmid constructs were verified by Sanger sequencing.

Cell Culture and Transfection. HEK 293SL cells (13) were propagated in plastic flasks and grown at 37 °C in 5% CO_2 and 90% humidity. HEK 293SL cells with targeted deletion of ARRB1 and ARRB2 (beta-arrestin knockout; ΔβARR1/2) were derived, authenticated, and propagated as previously described (14). Cells (350,000 in 1 mL) were transfected in suspension with 1.0 μg of plasmid DNA, complexed with linear PEI (molecular weight 25,000, 3:1 PEI:DNA ratio) and seeded (3.5×10^4 cells/well) in white 96-well plates. All cell lines were regularly tested for mycoplasma contamination.

Confocal Imaging. Cells grown on 25-mm round coverslips were transfected with FLAG-AT_1R, NES-Venus-mGsq, and Cerulean-RAB5A at a 2:1:1 ratio (2 μg DNA total per coverslip). After 24 h, 100 nM AngII was added to the growth medium, and cells were returned to the incubator at 37 °C for 15 min. Coverslips were transferred to an imaging chamber and imaged in D-PBS containing 100 nM AngII (Fig. 1*A*). Alternatively, untreated coverslips were washed in D-PBS and transferred to a heated stage maintained at 35 °C and imaged every 30 s for 18 min. After a 3-min control period, 100 nM AngII was added (*SI Appendix*, Fig. S1). Confocal images were acquired using a Leica SP8 scanning confocal microscope and a 63×, 1.4 numerical aperture objective. Venus was excited with a 488-nm diode laser and detected at 510 to 590 nm. Cerulean was excited with a 448-nm diode laser and detected at 455 to 500 nm.

BRET Assays.

Receptor trafficking. Parental HEK 293SL and ΔβARR1/2 cells were transfected with M_3R-*R*luc8 or AT_1R-*R*lucII and rGFP-CAAX or rGFP-FYVE. After a 48 h incubation, cells were washed once with Tyrode's buffer (140 mM NaCl, 2.7 mM KCl, 1 mM $CaCl_2$, 12 mM $NaHCO_3$, 5.6 mM D-glucose, 0.5 mM $MgCl_2$, 0.37 mM NaH_2PO_4, and 25 mM Hepes [pH 7.4]) and maintained in the same buffer. Cells were stimulated with agonist for 15 min or 1 h for AT_1R and

M_3R, respectively, before BRET measurements. Prior to BRET measurements, cells were incubated with coelenterazine 400a (5 min) for AT_1R-*R*lucII and coelenterazine h (10 min) for M_3R-*R*luc8.

G protein trafficking. HEK293T, parental HEK 293SL, or ΔβARR1/2 cells were transfected with either FLAG-AT_1R, HA-M_3R, B_2R, or OXTR, along with $G\alpha_q$-118-*R*lucII, $G\beta_1$, and $G\gamma_1/G\gamma_2$, in combination with rGFP-CAAX (PM), rGFP-FYVE (EE), rGFP-Giantin (GA), or rGFP-PTP1B (ER). After a 48-h incubation, cells were washed once with Tyrode's buffer and maintained in the same buffer. Cells were stimulated with agonist for 15 min before BRET measurements. Prior to BRET measurements, cells were incubated with coelenterazine 400a (5 min) or Prolume Purple (6 min).

Translocation of active G protein biosensors. HEK293T, parental HEK 293SL, or ΔβARR1/2 cells were transfected with either FLAG-AT_1R, HA-M_3R, B_2R, OXTR, or HA-TPαR, along with $G\alpha_q$, $G\alpha_{11}$, $G\alpha_{14}$, $G\alpha_{15}$, $G\alpha_{12}$, or $G\alpha_{13}$, p63RhoGEF-*R*lucII, and either rGFP-CAAX or rGFP-FYVE. Organelle inhibition was achieved by cotransfection with RGS-CAAX or RGS-FYVE. After a 48-h incubation, cells were washed once with Tyrode's buffer and maintained in the same buffer. Cells were stimulated with agonist for 5 min when looking at rGFP-CAAX and 15 min when looking at rGFP-FYVE before BRET measurements. Prior to BRET measurements, cells were incubated with coelenterazine 400a (5 min) or Prolume Purple (6 min).

Translocation of GRK2. HEK 293SL cells were transfected with FLAG-AT_1R or HA-M_3R, G_q, GRK2-D110A-*R*lucII, and rGFP-CAAX or rGFP-FYVE. After a 48-h incubation, cells were washed once with Tyrode's buffer and maintained in the same buffer. Cells were stimulated with AngII (10 μM) or ACh (100 μM), and BRET was measured immediately for rGFP-CAAX or after 15 min for rGFP-FYVE. Prior to BRET measurements, cells were incubated for 5 min with coelenterazine 400a.

Translocation of C1B. HEK 293SL cells were transfected with FLAG-AT_1R or HA-TPαR, *R*lucII-C1B, and rGFP-CAAX or rGFP-FYVE. After a 48-h incubation, cells were washed once with Tyrode's buffer and maintained in the same buffer. Cells were stimulated with AngII (100 nM) or U46619 (100 nM), and BRET was measured every 10 s for 400 to 600 s. Prior to BRET measurements, cells were incubated for 6 min with Prolume Purple.

Translocation of β-arrestin2. HEK 293SL cells were transfected with FLAG-AT_1R, β-arrestin2-*R*lucII, and rGFP-CAAX. After a 48-h incubation, cells were washed once with Tyrode's buffer and maintained in the same buffer. Cells were stimulated with AngII and BRET was measured after incubation with coelenterazine 400a (5 min).

BRET measurements. Plates were read on a Tecan Spark multimode microplate reader, Mithras LB 940 microplate reader, Tristar^2 LB 942 from Berthold Technologies, or VICTOR *X* Light multilabel plate reader from PerkinElmer, equipped with filters for BRET^2 [400/70 nm (donor) and 515/20 nm (acceptor)] and BRET^1 [480/20 nm (donor) and 530/20 nm (acceptor)], for detecting the *R*lucII (donor) and rGFP (acceptor) light emissions, respectively.

Luminescence Microscopy (BRET Imaging). A total of 2 to 3 × 10^5 HEK 293 cells (cultured with 10% NCS) were seeded into poly-D-lysine–coated MatTek 35-mm glass-bottom culture dishes (P35GC-1.5-14-C). Cells were cultured for 24 h and transfected with 1.0 μg DNA and 3 μL X-tremeGENE 9 transfection reagent. Cells were cultured for another 24 h and BRET imaging done as described previously (15). Images were generated by integrating photon counting images until the signal intensity of the pixel showing the highest value reached 100 photon counts.

Exposure time was 100 ms for each image, and image integration proceeded until sufficient signal intensity was obtained. A single image typically required 300 to 5,000 photon-counting images. Images in *SI Appendix*, Fig. S5 were treated with variance-stabilizing transformation–based Poisson denoising algorithm (49).

Data Analysis. Data analysis was performed using GraphPad Prism 8.4.0 (GraphPad Software). Quantitative data are expressed as the mean, and error bars represent the SEM, unless otherwise indicated. Curve fitting was performed by three or four parameter nonlinear regression. Statistical analyses were performed using one-sample *t* test, unpaired *t* test, one-way ANOVA, or two-way ANOVA.

Data Availability. mG probes are available from N.A.L. upon request. Some of the biosensors used in the present study are protected by patents, but all are available for academic research under regular material transfer agreement upon request to M.B. All other study data are included in the article and/or supporting information.

ACKNOWLEDGMENTS. We thank Monique Lagacé for critical reading of the manuscript. S.C.W. is supported by a fellowship from the Swedish Society for Medical Research (P18-0098); L.T.P.-e.-S. holds a Young Researcher grant from FAPESP (2016/24120-3); S.M.-L. is supported by a Vanier Canada Graduate Scholarship from the Canadian Institutes of Health Research (CIHR); N.A.L. is supported by NIH grant GM130142; and M.B. is funded by the CIHR (FDN-148431) and holds a Canada Research Chair in Signal Transduction and Molecular Pharmacology.

1. R. J. Lefkowitz, G protein-coupled receptors. III. New roles for receptor kinases and beta-arrestins in receptor signaling and desensitization. *J. Biol. Chem.* **273**, 18677–18680 (1998).
2. B. Plouffe, A. R. B. Thomsen, R. Irannejad, Emerging role of compartmentalized G protein-coupled receptor signaling in the cardiovascular field. *ACS Pharmacol. Transl. Sci.* **3**, 221–236 (2020).
3. B. R. Martin, N. A. Lambert, G. Activated, Activated G protein Gαs samples multiple endomembrane compartments. *J. Biol. Chem.* **291**, 20295–20302 (2016).
4. J. Z. Yu, M. M. Rasenick, Real-time visualization of a fluorescent G(alpha)(s): Dissociation of the activated G protein from plasma membrane. *Mol. Pharmacol.* **61**, 352–359 (2002).
5. R. Irannejad *et al.*, Conformational biosensors reveal GPCR signalling from endosomes. *Nature* **495**, 534–538 (2013).
6. D. D. Jensen *et al.*, Neurokinin 1 receptor signaling in endosomes mediates sustained nociception and is a viable therapeutic target for prolonged pain relief. *Sci. Transl. Med.* **9**, eaal3447 (2017).
7. J. H. Yoo *et al.*, ARF6 is an actionable node that orchestrates oncogenic GNAQ signaling in uveal melanoma. *Cancer Cell* **29**, 889–904 (2016).
8. N. N. Jimenez-Vargas *et al.*, Protease-activated receptor-2 in endosomes signals persistent pain of irritable bowel syndrome. *Proc. Natl. Acad. Sci. U.S.A.* **115**, E7438–E7447 (2018).
9. A. Manglik, B. K. Kobilka, J. Steyaert, Nanobodies to study G protein-coupled receptor structure and function. *Annu. Rev. Pharmacol. Toxicol.* **57**, 19–37 (2017).
10. R. Irannejad *et al.*, Functional selectivity of GPCR-directed drug action through location bias. *Nat. Chem. Biol.* **13**, 799–806 (2017).
11. B. Carpenter, R. Nehmé, T. Warne, A. G. Leslie, C. G. Tate, Structure of the adenosine A(2A) receptor bound to an engineered G protein. *Nature* **536**, 104–107 (2016).
12. Q. Wan *et al.*, Mini G protein probes for active G protein-coupled receptors (GPCRs) in live cells. *J. Biol. Chem.* **293**, 7466–7473 (2018).
13. Y. Namkung *et al.*, Monitoring G protein-coupled receptor and β-arrestin trafficking in live cells using enhanced bystander BRET. *Nat. Commun.* **7**, 12178 (2016).
14. L. M. Luttrell *et al.*, Manifold roles of β-arrestins in GPCR signaling elucidated with siRNA and CRISPR/Cas9. *Sci. Signal.* **11**, eaat7650 (2018).
15. H. Kobayashi, L. P. Picard, A. M. Schönegge, M. Bouvier, Bioluminescence resonance energy transfer-based imaging of protein-protein interactions in living cells. *Nat. Protoc.* **14**, 1084–1107 (2019).
16. K. B. Hubbard, J. R. Hepler, Cell signalling diversity of the Gqalpha family of heterotrimeric G proteins. *Cell. Signal.* **18**, 135–150 (2006).
17. C. Avet *et al.*, Selectivity landscape of 100 therapeutically relevant GPCR profiled by an effector translocation-based BRET platform. *bioRxiv* [Preprint] (2020). 10.1101/2020.04.20.052027 (Accessed 21 April 2020).
18. G. Milligan, E. Kostenis, Heterotrimeric G-proteins: A short history. *Br. J. Pharmacol.* **147** (suppl. 1), S46–S55 (2006).
19. S. Lutz *et al.*, Structure of Galphaq-p63RhoGEF-RhoA complex reveals a pathway for the activation of RhoA by GPCRs. *Science* **318**, 1923–1927 (2007).
20. R. J. Rojas *et al.*, Galphaq directly activates p63RhoGEF and Trio via a conserved extension of the Dbl homology-associated pleckstrin homology domain. *J. Biol. Chem.* **282**, 29201–29210 (2007).
21. L. A. Borden, R. Einstein, C. A. Gabel, F. R. Maxfield, Acidification-dependent dissociation of endocytosed insulin precedes that of endocytosed proteins bearing the mannose 6-phosphate recognition marker. *J. Biol. Chem.* **265**, 8497–8504 (1990).
22. Y. B. Hu, E. B. Dammer, R. J. Ren, G. Wang, The endosomal-lysosomal system: From acidification and cargo sorting to neurodegeneration. *Transl. Neurodegener.* **4**, 18 (2015).
23. K. Cotter, L. Stransky, C. McGuire, M. Forgac, Recent insights into the structure, regulation, and function of the V-ATPases. *Trends Biochem. Sci.* **40**, 611–622 (2015).
24. N. Bayer *et al.*, Effect of bafilomycin A1 and nocodazole on endocytic transport in HeLa cells: Implications for viral uncoating and infection. *J. Virol.* **72**, 9645–9655 (1998).
25. C. V. Carman *et al.*, Selective regulation of Galpha(q/11) by an RGS domain in the G protein-coupled receptor kinase, GRK2. *J. Biol. Chem.* **274**, 34483–34492 (1999).
26. D. M. Berman, A. G. Gilman, Mammalian RGS proteins: Barbarians at the gate. *J. Biol. Chem.* **273**, 1269–1272 (1998).
27. M. D. Hains, D. P. Siderovski, T. K. Harden, Application of RGS box proteins to evaluate G-protein selectivity in receptor-promoted signaling. *Methods Enzymol.* **389**, 71–88 (2004).
28. I. Masuho *et al.*, A global map of G protein signaling regulation by RGS proteins. *Cell* **183**, 503–521.e19 (2020).
29. A. Beautrait *et al.*, Mapping the putative G protein-coupled receptor (GPCR) docking site on GPCR kinase 2: Insights from intact cell phosphorylation and recruitment assays. *J. Biol. Chem.* **289**, 25262–25275 (2014).

30. D. E. Logothetis, Y. Kurachi, J. Galper, E. J. Neer, D. E. Clapham, The beta gamma subunits of GTP-binding proteins activate the muscarinic K+ channel in heart. *Nature* **325**, 321–326 (1987).
31. W. J. Tang, A. G. Gilman, Type-specific regulation of adenylyl cyclase by G protein beta gamma subunits. *Science* **254**, 1500–1503 (1991).
32. R. Sterne-Marr *et al*., G protein-coupled receptor Kinase 2/G alpha q/11 interaction. A novel surface on a regulator of G protein signaling homology domain for binding G alpha subunits. *J. Biol. Chem.* **278**, 6050–6058 (2003).
33. N. G. Tsvetanova, R. Irannejad, M. von Zastrow, G protein-coupled receptor (GPCR) signaling via heterotrimeric G proteins from endosomes. *J. Biol. Chem.* **290**, 6689–6696 (2015).
34. A. R. B. Thomsen *et al*., GPCR-G protein-β-arrestin super-complex mediates sustained G protein signaling. *Cell* **166**, 907–919 (2016).
35. A. H. Nguyen *et al*., Structure of an endosomal signaling GPCR-G protein-β-arrestin megacomplex. *Nat. Struct. Mol. Biol.* **26**, 1123–1131 (2019).
36. A. K. Shukla *et al*., Visualization of arrestin recruitment by a G-protein-coupled receptor. *Nature* **512**, 218–222 (2014).
37. A. M. Lyon, V. G. Taylor, J. J. Tesmer, Strike a pose: Gαq complexes at the membrane. *Trends Pharmacol. Sci.* **35**, 23–30 (2014).
38. M. Fernandez-Borja, L. Janssen, D. Verwoerd, P. Hordijk, J. Neefjes, RhoB regulates endosome transport by promoting actin assembly on endosomal membranes through Dia1. *J. Cell Sci.* **118**, 2661–2670 (2005).
39. A. Bondar, W. Jang, E. Sviridova, N. A. Lambert, Components of the G_s signaling cascade exhibit distinct changes in mobility and membrane domain localization upon β_2 -adrenergic receptor activation. *Traffic* **21**, 324–332 (2020).
40. A. M. Lazar *et al*., G protein-regulated endocytic trafficking of adenylyl cyclase type 9. *eLife* **9**, e58039 (2020).
41. J. R. Lane, L. T. May, R. G. Parton, P. M. Sexton, A. Christopoulos, A kinetic view of GPCR allostery and biased agonism. *Nat. Chem. Biol.* **13**, 929–937 (2017).
42. P. D. Ramírez-García *et al*., A pH-responsive nanoparticle targets the neurokinin 1 receptor in endosomes to prevent chronic pain. *Nat. Nanotechnol.* **14**, 1150–1159 (2019).
43. E. Goupil *et al*., Angiotensin II type I and prostaglandin F2α receptors cooperatively modulate signaling in vascular smooth muscle cells. *J. Biol. Chem.* **290**, 3137–3148 (2015).
44. J. L. Parent, P. Labrecque, M. J. Orsini, J. L. Benovic, Internalization of the TXA2 receptor alpha and beta isoforms. Role of the differentially spliced cooh terminus in agonist-promoted receptor internalization. *J. Biol. Chem.* **274**, 8941–8948 (1999).
45. R. Schrage *et al*., The experimental power of FR900359 to study Gq-regulated biological processes. *Nat. Commun.* **6**, 10156 (2015).
46. N. Okashah *et al*., Agonist-induced formation of unproductive receptor-G_{12} complexes. *Proc. Natl. Acad. Sci. U.S.A.* **117**, 21723–21730 (2020).
47. J. Quoyer *et al*., Pepducin targeting the C-X-C chemokine receptor type 4 acts as a biased agonist favoring activation of the inhibitory G protein. *Proc. Natl. Acad. Sci. U.S.A.* **110**, E5088–E5097 (2013).
48. Y. Namkung *et al*., Functional selectivity profiling of the angiotensin II type 1 receptor using pathway-wide BRET signaling sensors. *Sci. Signal.* **11**, eaat1631 (2018).
49. L. Azzari, A. Foi, Variance stabilization for Noisy+Estimate combination in iterative Poisson denoising. *IEEE Signal Process. Lett.* **23**, 1086–1090 (2016).